Mesolytic Cleavage of the O–CO Bond in Enol Acetate Cation Radicals with Direct Formation of α-Carbonyl Cations. Mechanistic and Synthetic Aspects[1]

Michael Schmittel,* Jürgen Heinze,† and Holger Trenkle

Institut für Organische Chemie, Universität Würzburg, Am Hubland, 97074 Würzburg, FRG, and Institut für Physikalische Chemie der Universität Freiburg, Albertstr. 21, 79104 Freiburg, FRG

Received December 29, 1994[⊗]

For the first time, enol ester cation radicals are reversibly monitored in a cyclic voltammetry experiment. Preparative one-electron oxidation of enol acetates **A1**–**A4** leads to the formation of benzofurans **B1**–**B4** through mesolytic O–CO bond fragmentation to α-carbonyl cations and the acetyl radical. With **A3**$^{\bullet+}$, the kinetics of the O–CO bond cleavage was investigated by cyclic voltammetry, providing $\Delta H^{\ddagger} = 17.0$ kcal mol^{-1} and $\Delta S^{\ddagger} = 11$ cal mol^{-1} K^{-1} in dichloromethane. The slightly increased rate of bond dissociation upon addition of acetonitrile is explained with charge localization in the transition state rather than with a solvent-assisted bond cleavage mechanism. The occurrence of curve crossings and isopotential points in the cyclic voltammograms of the model compounds **A1**–**A4** at low scan rates can be rationalized by a multiparameter reaction scheme based on an ECCE$_{DISP}$ mechanism, digital simulation of which confirmed the cleavage selectivity and allowed for the determination of the involved rate constants of the homogeneous chemical reaction steps.

Introduction

While homolytic and heterolytic bond dissociation data have contributed in a paramount way to our present understanding of chemical reactivity, very little is known, particularly in solution, about mesolytic[2] bond cleavage reactions.[3] Moreover, mesolytic bond cleavage reactions offer an exceptional potential for triggering intriguing synthetic transformations in all fields of organic chemistry because of the vastly reduced activation barrier for bond dissociation in odd-electron molecules in numerous cases. By developing a constant, optimized electrophoric group which can be oxidized or reduced at low potentials, cleavage reactions may be carried out chemoselectively in the presence of many other functional groups.[4] Hence, this straightforward concept can be readily envisaged gaining widespread importance in protecting group chemistry. However, although some important aspects of mesolytic bond cleavage reactions have been emerging just recently, much more knowledge is needed about thermodynamic and kinetic data.[2,3]

Therefore, we have started a research project to investigate the potential of the enol ester functionality as an electroactive protecting group for carbonyl compounds since, by the manipulation of the ester moiety, various possibilities should exist to influence the O–CO bond dissociation barrier, some aspects of which will be described herein. Interestingly, O–CO bond dissociation in enol ester cation radicals has not been directly observed in solution so far. An indication for this reaction path was only recently provided in the oxygenation of enol acetates of phenyl propiophenones under PET conditions that afforded the corresponding ketones, presumably formed by O–CO bond cleavage of the corresponding enol acetate cation radicals.[5] However, in the vast majority of other investigations, conducted usually under anodic oxidation conditions, formation of α-acetoxy ketones and α,β-unsaturated ketones was registered, e.g. in acetic acid.[6] These products could readily be explained by deprotonation or nucleophilic attack being the primary steps of the reaction sequence, thus indicating that O–CO bond cleavage cannot compete with the other reaction pathways.

In order to make O–CO bond cleavage the unique reaction pathway in enol ester cation radicals and to gain insight into the fragmentation rates, we decided to study model compounds that by their particular structure would prevent deprotonation and nucleophilic attack from being competitive reaction pathways. These requirements led us to investigate the acetates **A1**–**A4** since they lack γ-protons, and the effective shielding of the β-position by two bulky mesityl groups should prevent any attack of nucleophiles on the cation radical.

Results

All model compounds showed irreversible oxidation potentials in the range of 1.0–1.2 V vs ferrocene/

† Institut für Physikalische Chemie der Universität Freiburg.

⊗ Abstract published in *Advance ACS Abstracts,* April 15, 1995.

(1) Electroactive Protecting Groups and Reaction Units, part 1.

(2) The expression mesolytic has been coined by Maslak and will be used throughout this paper: Maslak, P.; Narvaez, J. N. *Angew. Chem.* **1990**, *102*, 302; *Angew. Chem., Int. Ed. Engl.* **1990**, *29*, 283.

(3) Some recent references for mesolytic bond cleavage in cation radicals: (a) Maslak, P.; Asel, S. *J. Am. Chem. Soc.* **1988**, *110*, 8260. (b) Dinnocenzo, J. P.; Farid, S.; Goodman, J. L.; Gould, I. R.; Todd, W. P.; Mattes, S. L. *J. Am. Chem. Soc.* **1989**, *111*, 8973. (c) Camaioni, D. M. *J. Am. Chem. Soc.* **1990**, *112*, 9475. (d) Popielarz, R.; Arnold, D. R. *J. Am. Chem. Soc.* **1990**, *112*, 3068. (e) Saeva, F. D. *Top. Curr. Chem.* **1990**, *156*, 59. (f) Ci, X.; Kellet, M. A.; Whitten, D. G. *J. Am. Chem. Soc.* **1991**, *113*, 3893. (g) Arnett, E. M.; Flowers, R. A. *Chem. Soc. Rev.* **1993**, 9. (h) Perrier, S.; Sankararaman, S.; Kochi, J. K. *J. Chem. Soc., Perkin Trans. 2* **1993**, 825. (i) Maslak, P.; Vallombroso, T. M.; Chapman, W. H., Jr.; Narvaez, J. N. *Angew. Chem.* **1994**, *106*, 110. (j) Adam, W.; Miranda, M. A.; Mojarrad, F.; Sheikh, H. *Chem. Ber.* **1994**, *127*, 875.

(4) Gassman, P. G.; Bottorf, K. J. *J. Am. Chem. Soc.* **1988**, *110*, 1097.

(5) Algarra, F.; Baldoví, M. V.; García, H.; Miranda, M. A.; Primo, J. *Monatsh. Chem.* **1993**, *124*, 209.

(6) (a) Shono, T.; Matsumara, Y.; Nakagawa, Y. *J. Am. Chem. Soc.* **1974**, *96*, 3532. (b) Shono, T.; Okawa, M.; Nishiguchi, I. *J. Am. Chem. Soc.* **1975**, *97*, 6144. (c) Shono, T.; Nishiguchi, I.; Kashimura, S.; Okawa, M. *Bull. Chem. Soc. Jpn.* **1987**, *51*, 2181.

(7) All potentials are referenced to the ferrocene/ferrocenium (Fc) couple unless otherwise noted. To obtain values vs SCE, simply add +0.39 V.

0022-3263/95/1960-2726$09.00/0

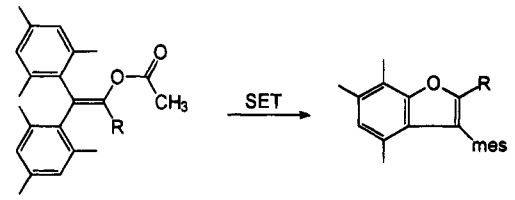

Figure 1. Products of the one-electron oxidation of **A1–A4** (mes = mesityl = 2,4,6-trimethylphenyl).

Chart 1. Model Compounds and Their Irreversible Peak Potentials[a]

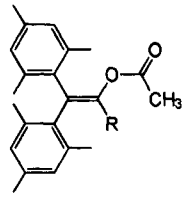

R	H	CH_3	tBu	Ph
	A1	**A2**	**A3**	**A4**
E_{pa}[a]	1.19	1.20	1.16	1.04

[a] 10^{-3} M in acetonitrile containing 0.1 M Bu_4NPF_6. [V] vs Fc.

Table 1. Preparative One-Electron Oxidation of A1–A4

enol acetate	oxidant	oxidant (equiv)	benzofuran[a]	mass balance[b]
A1	TBPA	1	6	72
A1	TBPA	2	2	64
A2	TBPA	1	19	54
A2	TBPA	2	5	49
A3	TBPA	1	9	23
A3	TBPA	2	7	60
A3	$Fe(phen)_3^{3+}$	1	52	73
A3	$Fe(phen)_3^{3+}$	2	41	97
A3	TPC	1	47	91
A3	TPC	0.3	52	79
A3	TPC	0.2	47	83
A4	TBPA	1	13	88
A4	TBPA	2	32	67

[a] Based on oxidation equivalents. [b] Based on starting enol acetate.

ferrocenium[7] (Fc) at 100 mV s^{-1} (Chart 1). This is within an acceptable range where both chemical one-electron oxidation reactions and photoinduced electron transfer initiation can be realized in the presence of many other common functional groups.[4]

Preparative one-electron oxidation of enol acetates **A1–A4** by tris(4-bromophenyl)aminium hexachloroantimonate (TBPA, $E_{1/2}$ = 0.73 V), tris(1,10-phenanthroline)iron(III) hexafluorophosphate ($Fe(phen)_3^{3+}$, $E_{1/2}$ = 0.76 V), or thianthrenium perchlorate (TPC, $E_{1/2}$ = 0.95 V) afforded benzofurans **B1–B4** (Figure 1 and Table 1). In the case of TBPA being the oxidant, the benzofurans partially underwent further reactions to yield monobrominated benzofurans as detected by GC–MS.

Cyclic Voltammetry Studies. Cyclic voltammetric investigation of enol acetates **A1–A4** displayed irreversible oxidation waves that exhibited a linear shift of the anodic peak potential with log v and a decreasing ratio $I_{pa}/v^{1/2}$ with an increasing scan rate. These diagnostic criteria point to the occurrence of a reversible electron transfer, followed by a fast irreversible chemical reaction[8] involving a further electron transfer reaction.

Curve-Crossing Effects. In addition, an intriguing curve crossing in the reverse scan, which decreased with an increasing scan rate, was observed at low scan rates

(8) Nicholson, R. S.; Shain, I. *Anal. Chem.* **1964**, *36*, 706.

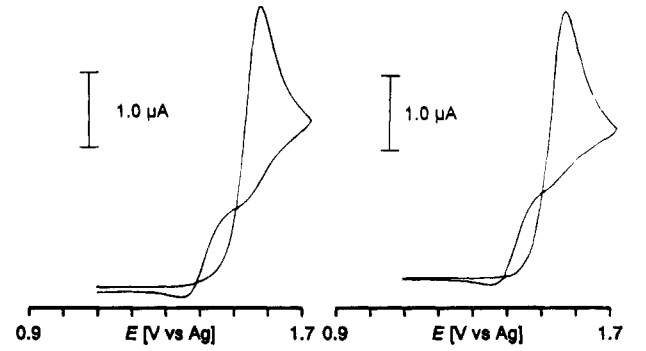

Figure 2. Cyclic voltammogram of **A3** at 50 mV s^{-1}, 10^{-3} M in acetonitrile containing 0.1 M Bu_4NPF_6. Left, experiment; right, digital simulation.

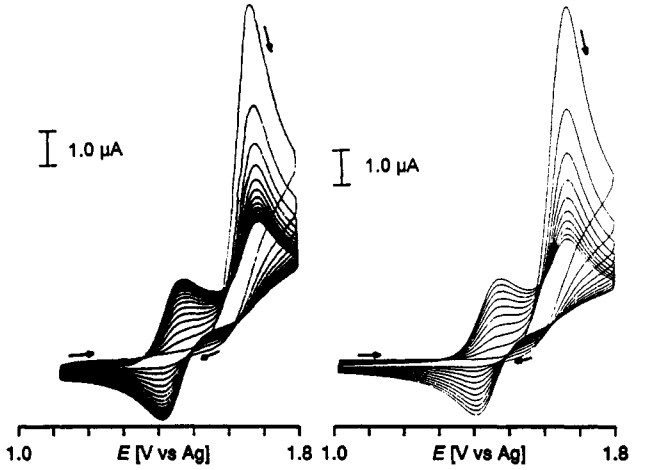

Figure 3. Benzofuran formation in the multisweep cyclic voltammogram of **A3** at 500 mV s^{-1}, 10^{-3} M in acetonitrile containing 0.1 M Bu_4NPF_6. Left, experiment; right, digital simulation.

for all systems (Figure 2). A closer investigation revealed that this rare phenomenon[9] depended on the concentration of the involved electroactive species, thus indicating slow formation of an easily oxidizable followup product under participation of a homogeneous disproportionation equilibrium.[10] This second electron transfer step causes a superimposal anodic current, decreasing in the same manner as the concentration of the followup product when the time scale of the experiment is reduced at faster scan rates. This behavior is reflected in the diagnostic criteria concerning the dependence of the anodic peak current from the scan rate.[8]

In multisweep experiments, the followup products of **A1–A4** gave rise to reversible waves (except for **A1**) at lower oxidation potentials (Figure 3), with formal redox potentials all around 0.9 V vs Fc. By explicit comparison of those with the redox potentials of authentic samples of the benzofurans **B2–B4** (Table 2), the unknown products in the cyclic voltammogram (CV) could be unequivocally assigned to the benzofurans **B2–B4**.

Digital Simulation. Digital simulation of the cyclic voltammograms using the implicit Crank–Nicholson technique[11] showed good agreement with experimental

(9) (a) Kuchynka, D. J.; Kochi, J. K. *Inorg. Chem.* **1988**, *27*, 2574. (b) Hinkelmann, K.; Heinze, J.; Schacht, H.-T.; Field, J. S.; Vahrenkamp, H. *J. Am. Chem. Soc.* **1989**, *111*, 5078.

(10) Amatore, C.; Pinson, J.; Saveant, J. M.; Thiebault, A. *J. Electroanal. Chem. Interfacial Electrochem.* **1980**, *107*, 59.

Table 2. Redox Potentials of Benzofurans B2–B4[a]

benzofuran	$E°$ (V)
B2	0.91
B3	0.93
B4	0.84

[a] Versus Fc, 10^{-3} M in acetonitrile containing 0.1 M Bu_4NPF_6.

curves when based on an $ECCE_{DISP}$ mechanism (Figures 2–4). Accordingly, cation radical **A3**$^{\bullet+}$ undergoes fast fragmentation with $k_{f1} > 1000$ s^{-1} to an α-carbonyl cation and an acetyl radical. In addition, a rate constant $k_{f2} = 0.08$ s^{-1} for the overall reaction of the α-carbonyl cation to the benzofuran **B3** was derived from the simulation. The latter rate constant could be independently verified through a CV investigation of enol **E3** since, in this system, the partially reversible wave of **B3** could be detected after the irreversible oxidation wave of **E3**. Characteristically, the intensity of the wave of **B3** decreased with an increasing scan rate. Digital simulation of these curves afforded a rate constant of $k_{f2} = 0.1$ s^{-1} for the rate-determining step of the overall reaction of the α-carbonyl cation to the benzofuran **B3** which is in good accordance with the one determined by the examination of the enol acetate CV.

A sensitive tool for verifying the data obtained from the curve-crossing experiments is simulation of the multisweep experiment, a fingerprint of the complex interactions between the electroactive and chemically reactive species. As the number of scans increases, a dynamic equilibrium is composed in the diffusion layer in which oxidation of **A3** and subsequent reactions form exactly the same amount of **B3** as is drawn off by diffusion. The relative current intensities are directly proportional to the concentration of the involved species, and accordingly, a characteristic reflection of concentration profiles occurs. The occurrence of four isopotential points[12] indicates that one electroactive species was quantitatively converted into another, the sum of reactant and product concentrations thus remaining constant.[9] Besides the number and position of isopotential points, the decrease of the anodic peak current of **A3** and the increase of the anodic current of **B3** with the number of cycles are very characteristic properties of the multisweep CV. Consequently, they can be used to fit the rate constants since only small variations result in a completely different behavior of the simulated spectrum.

To perform the simulation, the three reaction steps of the α-carbonyl cation leading to benzofuran **B3** (Figure 10) were combined into one overall reaction with the rate constant k_{f2}.

Fast Scan Cyclic Voltammetry at Ultramicroelectrodes. At fast scan rates (>5000 V s^{-1}), a reduction wave of the enol acetate cation radical **A3**$^{\bullet+}$ could be observed in acetonitrile, indicative of a fast followup reaction with a first-order rate constant on the order of $\approx 2 \times 10^4$ s^{-1}. The occurrence of capacitive currents and iR drop effects at fast scan rates prevented a closer determination of the rate constant for O–CO bond dissociation. In dichloromethane, **A3** already showed

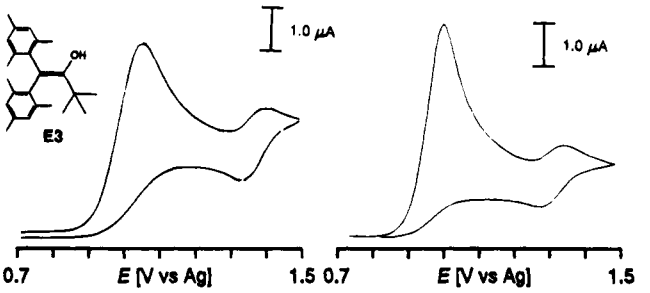

Figure 4. Cyclic voltammogram of the enol **E3** at 50 mV s^{-1}, 10^{-3} M in acetonitrile containing 0.1 M Bu_4NPF_6. Left, experiment; right, digital simulation.

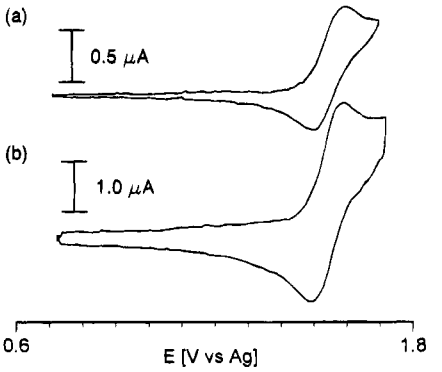

Figure 5. Fast scan cyclic voltammogram of **A3** at (a) 100 and (b) 1750 V s^{-1}, 0.02 M in dichloromethane containing 0.2 M Bu_4NPF_6 at a 25 μm gold disk electrode.

partially reversible redox waves at scan rates of >20 V s^{-1}. Fully reversible CVs were obtained at scan rates of >1500 V s^{-1} (Figure 5). This represents the first direct observation of an enol ester cation radical in solution in an electrochemical experiment, allowing for the determination of the thermodynamically relevant redox potential of **A3** ($E_{1/2} = 1.16$ V vs Fc).

At fast scan rates, benzofuran formation cannot be observed any longer in the electrochemical experiment. According to the slow rate constant of benzofuran formation from the cyclized intermediate ($k_{f2} = 0.1$ s^{-1}), the complex $ECCE_{DISP}$ behavior at low scan rates is consequently reduced to an EC_{irr} mechanism when going to higher scan rates. The kinetics of this type of reaction scheme can easily be examined since it is readily characterized by the following typical diagnostic criteria. The ratio $I_a/v^{1/2}$ decreases with an increasing v, and the ratio of cathodic to anodic peak current I_{pc}/I_{pa} asymptotically approaches at high scan rates, independent of the concentration, the theoretical value of 1, indicative of a fully reversible one-electron oxidation process.

The kinetic analysis of the cyclic voltammograms between 100 and 1000 V s^{-1} was performed according to the method of Nicholson and Shain[8] using a working curve for an EC_{irr} mechanism to provide a first-order rate constant for the fragmentation reaction of 110 s^{-1} (Figure 6). This value could likewise be confirmed by digital simulation based on the complete $ECCE_{DISP}$ mechanism.

Likewise, the observation of the enol ester cation radical was possible at low temperatures in dichloromethane. Below −20 °C, a reduction wave began to develop at scan rates of ≤500 mV s^{-1}. The kinetics were examined in the previously described way at temperatures between −36 and −46 °C, providing first-order rate constants of 0.10–0.15 s^{-1}. An Eyring plot based on the

(11) (a) Lasia, A. *J. Electroanal. Chem. Interfacial Electrochem.* **1983**, *146*, 397. (b) Heinze, J.; Störzbach, M.; Mortensen, J. *J. Electroanal. Chem. Interfacial Electrochem.* **1984**, *165*, 61. (c) Heinze, J.; Störzbach, M. *J. Electroanal. Chem. Interfacial Electrochem.* **1993**, *346*, 1.

(12) (a) Unterecker, D. F.; Bruckenstein, S. *Anal. Chem.* **1972**, *44*, 1009. (b) Unterecker, D. F.; Bruckenstein, S. *J. Electroanal. Chem. Interfacial Electrochem.* **1974**, *57*, 77.

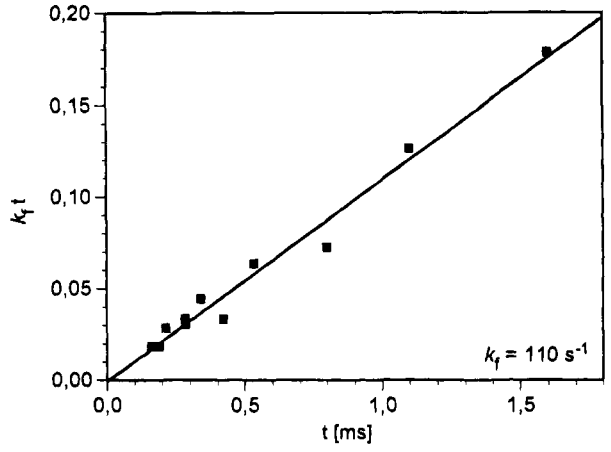

Figure 6. Kinetics of the mesolytic bond cleavage of **A3**$^{\bullet+}$. v = 100–1000 V s^{-1}, 0.02 M in dichloromethane containing 0.2 M Bu_4NPF_6.

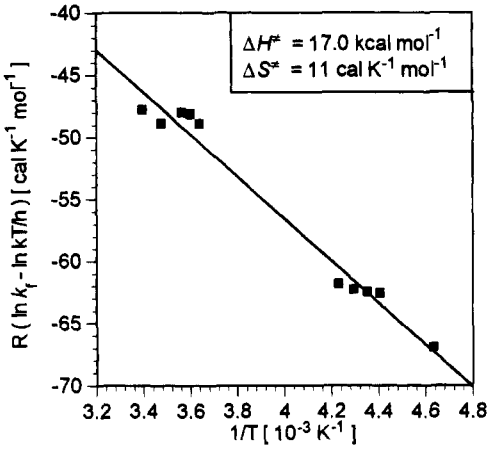

Figure 7. Eyring plot of the mesolytic O–CO bond cleavage in **A3**$^{\bullet+}$.

low-temperature measurements in addition to the results obtained by fast scan CV allowed for the determination of the activation parameters of the fragmentation reaction: $\Delta H^{\ddagger}$ = 17.0 kcal mol^{-1} and $\Delta S^{\ddagger}$ = 11 cal K^{-1} mol^{-1} (Figure 7).

Rate Constants in Dichloromethane/Acetonitrile Mixtures. Since direct determination of the first-order fragmentation constant in acetonitrile was not feasible with our instrumentation at low temperatures, we determined the rate constants in different dichloromethane/acetonitrile mixtures at −45 and −57 °C. A linear relationship resulted between the acetonitrile concentration and the obtained rate constants (Figure 8), which allowed for extrapolation to pure acetonitrile, providing rate constants of 1.87 s^{-1} at −45 °C and 0.75 s^{-1} at −57 °C, respectively. To some extent, confirmation of the reliability of this extrapolation method may be derived from the fact that the extrapolated rate constant for pure dichloromethane at −57 °C ($k_{DCM,\ -57°C}$ = 0.011 s^{-1}) lies on the straight line of the Eyring plot (Figure 7).

In addition, the investigations in dichloromethane supplied other useful information for understanding the reaction mechanism. A further irreversible oxidation wave with a characteristically slow heterogeneous electron transfer appeared at 1.85 V vs Fc, independent of the enol acetate that was studied. By an independent experiment, the oxidation potential of diacetyl whose formation can readily be rationalized by dimerization of

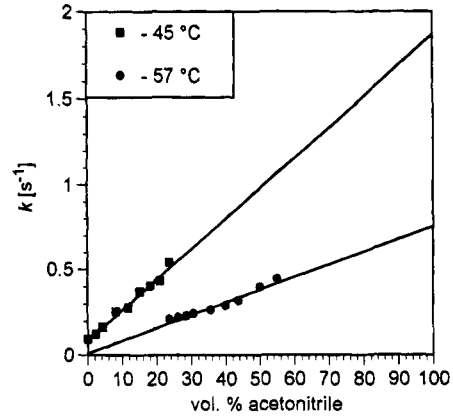

Figure 8. Rate constants in dichloromethane/acetonitrile mixtures at −45 and −57 °C.

acetyl radical at the electrode was determined to be 1.86 V vs Fc. As in the enol acetate oxidation, the wave of diacetyl was irreversible, showing very slow heterogeneous electron transfer. Furthermore, electrolysis of **A3**, followed by reaction with hydroxylamine and nickel(II) iodide, afforded a deeply red precipitate of nickel(II) diacetyldioxime, corroborating the formation of diacetyl from fragmentation of **A3**$^{\bullet+}$.

Discussion

Formation of benzofurans by one-electron oxidation of stable enols is known to proceed via an intermediate α-carbonyl cation which undergoes cyclization, [1,2]-methyl shift, and deprotonation.[13,14] The good agreement in the rate constant of the rate-determining step of benzofuran formation starting from either the enol or the enol acetate as shown by digital simulation of the cyclic voltammograms (Figures 2–4) consequently suggests that the same intermediate, namely the α-carbonyl cation, is common to both oxidations. Obviously, one-electron oxidation of enol esters **A1**–**A4** does result in mesolytic O–CO bond cleavage, thus providing a hitherto unknown way to α-carbonyl cation chemistry. However, formation of α-carbonyl cations may occur in two distinct ways, representative of the two selectivities for mesolytic cleavage (Figure 9). Accordingly, the α-carbonyl cation is formed directly either by fragmentation of the enol acetate cation radical (mechanistic scheme (Mech) B) or by the converse cleavage selectivity providing first an intermediate α-carbonyl radical which is immediately oxidized under our conditions (Mech A). The rapid, diffusion-controlled oxidation of eventually formed α-carbonyl radicals **R1**–**R4** would be obvious on the basis of their low oxidation potentials (E_p^{ox} (**R1**) = 0.36 V vs Fc, E_p^{ox} (**R2**) = 0.21 V vs Fc, E_p^{ox} (**R3**) = 0.14 V vs Fc, and E_p^{ox} (**R4**) = 0.24 V vs Fc).[14]

In principle, dissociative electron transfer could have been a third mechanistic alternative. However, this proposal can definitely be excluded because reversible waves were observed by using fast scan cyclic voltammetry, thus constituting direct evidence for the existence of an enol acetate cation radical as the intermediate of the oxidative cleavage reaction.

(13) Schmittel, M.; Gescheidt, G.; Röck, M. *Angew. Chem.* **1994**, *106*, 2056; *Angew. Chem., Int. Ed. Engl.* **1994**, *33*, 1961.
(14) Röck, M.; Schmittel, M. *J. Chem. Soc., Chem. Commun.* **1993**, 1739.
(15) Dewar, M. J. S.; Zoebisch, E. G.; Healy, E. F.; Stewart, J. J. P. *J. Am. Chem. Soc.* **1985**, *107*, 3902–3909.

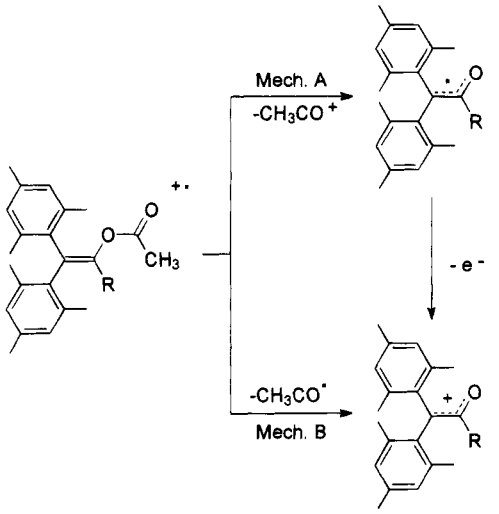

Figure 9. Formation of α-carbonyl cations.

Selectivity of the Mesolytic Cleavage. AM1 calculations[15] on the heats of formation of $\mathbf{A2}^{\bullet+}$ and the possible fragmentation products afforded a difference between the two cleavage mechanisms of 15 kcal/mol in favor of Mech B (to an α-carbonyl cation and an acetyl radical). Indeed, the same preference for bond cleavage selectivity can be verified in the gas phase by the fragmentation pattern in the mass spectral analysis. However, this finding does not necessarily have any direct bearing on the situation in the solution phase. Using a simple thermochemical cycle, it becomes obvious that the oxidation potential of the α-carbonyl radical vs the oxidation potential of the acetyl radical determines the cleavage selectivity in solution. The oxidation potential of the acetyl radical in acetonitrile can be approximated from the experimental ionization potential (IP = 8.05 eV) using Miller's[16] or Gassman's[17] correlation of $E_{1/2}$ vs IP, the two providing $E_{1/2}$ = 1.07 and 1.01 V, respectively. Comparing this potential to those of the α-carbonyl radicals would suggest that Mech B is preferred by about 15−20 kcal mol^{-1} in acetonitrile.

Experimental evidence for the cleavage according to Mech B in acetonitrile is provided by CV since no sufficient accordance of experimental and simulated data could be achieved either in the curve-crossing or in the multisweep experiments when we used the mechanistic scheme based on Mech A. Most importantly, the anodic peak currents at steady state concentrations in the multisweep experiment of both enol acetate **A3** and product **B3** are basically the same. Since removal of one electron from **B3** is known to provide $\mathbf{B3}^{\bullet+}$ reversibly, only one electron is equally removed from **A3**. In addition, comparison of the current intensities of the oxidation waves of **A3** with respect to the ferrocene/ferrocenium couple in acetonitrile demonstrated a I_{pa} (**A3**)/I_{pa} (Fc) at 50 mV s^{-1} of 1.06, strongly indicative of a one-electron transfer with a small superimposed benzofuran current, which is in good accordance with the diagnostic criteria.[18]

Additional experimental confirmation of Mech B was derived again from CV but is strictly limited to the system in dichloromethane. The appearance of a second irreversible oxidation wave at a potential of 1.85 V, independent of the employed enol acetate, points to the formation of the same electroactive species. Therefore, most likely, it has to be a product of the acetyl fragment. In line with our estimated $E_{1/2}$ for the acetyl radical, we don't expect the radical to be oxidized at the electrode, which proposes the formation of diacetyl through radical coupling. Direct evidence for the formation of diacetyl via mesolysis of the enol acetate cation radical **A3** was obtained by exhaustive electrolysis of **A3**, followed by reaction with hydroxylamine and nickel(II) iodide to yield a red complex of nickel(II) diacetyldioxime. On the other side, mesolysis according to Mech A should afford an acetyl cation which ought to be quenched by the solvent or by nucleophilic impurities.[19] Reduction of the acetyl cation to the radical is extremely unlikely in light of the high redox potential and the short lifetime of the involved species.

A further, although less stringent, corroboration for Mech B can be derived from the results of the one-electron oxidation. Formation of benzofuran, according to Mech A, requires 2 equiv of one-electron oxidant because of the additional oxidation step, while Mech B gets along with only 1 equiv of oxidant. Experimentally, the best yield with 1 equiv of oxidant was 50% of benzofuran; thus, according to Mech A, which requires 2 equiv of oxidant for benzofuran formation, it would be 100%. Since in most cases the mass balance was not approximately quantitative, this would necessarily imply that we lost only enol acetate but no benzofuran during workup. Unfortunately, all attempts to raise the benzofuran yield significantly beyond 50% failed. Since both primary products of the intermediate acetyl radical, namely acetaldehyde and diacetyl, proved stable to the oxidation conditions for our reaction times, we assume that hydrogen abstraction from acetonitrile produces α-cyano methyl radicals that dimerize to readily oxidizable ketene imines.[20]

Thus, all experimental evidence points to Mech B as the most likely pathway. For comparison, C−C bond cleavage of aryl alkyl ketone cation radicals provides arylmethyl cations and acetyl radicals but with a much higher rate constant.[21] Altogether, we would not expect our cleavage mechanism to change from B to A when switching the solvent from dichloromethane to acetonitrile since the differential solvation energies, as determined by the Born equation, are only in the region of 3−4 kcal mol^{-1}.

Rate Constants. The activation parameters in dichloromethane, in particular the slightly positive activation entropy, can be readily reconciled with Mech B since we expect the late transition state of O−CO dissociation to resemble the products. Conversely, according to Mech A, a cation radical with a large ion radius is cleaved into a large radical and a small cation with high charge density which would suggest strong localization of the positive charge at the breaking O−CO bond in the transition state, therefore resulting in a negative activation entropy. Indeed, this was observed in mesolytic bond cleavage reactions of bicumyl cation radicals.[2] Similarly,

(16) Miller, L. L.; Nordblom, G. D.; Mayeda, E. A. *J. Am. Chem. Soc.* **1972**, *94*, 916.
(17) Gassman, P. G.; Yamaguchi, R. *J. Am. Chem. Soc.* **1979**, *101*, 1308.
(18) The decreasing current intensity for **A3** relative to ferrocene with increasing scan rates reflects slow benzofuran formation on the time scale of the experiment.
(19) Becker, J. Y.; Miller, L. L.; Siegel, T. M. *J. Am. Chem. Soc.* **1975**, *97*, 849.
(20) Becker, J. Y.; Shakkour, E. *Tetrahedron* **1993**, *49*, 6285.
(21) Akaba, R.; Niimura, Y.; Fukushima, T.; Kawai, Y.; Tajima, T.; Kuragami, T.; Negishi, A.; Kamata, M.; Sakuragi, H.; Tokumaru, K. *J. Am. Chem. Soc.* **1992**, *114*, 4460.

the positive activation entropy precludes a solvent-assisted bond cleavage mechanism since, from Dinnocenzo's data[3b] on benzyltrialkylsilane$^{\bullet+}$ fragmentation, strongly negative activation entropies would be reasonable.

But what is the situation in acetonitrile? Although we have not been able to directly determine the rate constant of O–CO bond cleavage in acetonitrile at low temperatures, it can be adequately extrapolated from the experiments in dichloromethane/acetonitrile mixtures. Importantly, the bond dissociation in acetonitrile ($k_{AN,\ -45°C}$ = 1.85 s^{-1}) is always a more rapid process than in dichloromethane ($k_{DCM,\ -45°C}$ = 0.1 s^{-1}), proposing at first that acetonitrile may act as a nucleophile in the bond fragmentation. However, in light of the above arguments, it is difficult to write down a reasonable mechanistic proposal depicting nucleophilic attack on **A3**.$^{\bullet+}$ First, it is highly unlikely that acetonitrile attacks the β-position of the sterically encumbered enol moiety, which is supported by the fact that no products other than benzofurans **B1**–**B4** were found. Second, attack at the acetyl carbon should result in a reversed cleavage selectivity, which was definitely ruled out on the basis of the CV results. Neither do the CVs provide any hint for cleavage selectivity according to Mech A. Moreover, a much more pronounced rate acceleration (a factor of >4000) was observed when switching from dichloromethane to acetonitrile in the corresponding silyl enol ether system[22] where we have been able to unequivocally prove the nucleophile-assisted bond cleavage through the addition of various alcohols. Hence, we propose that the moderate acceleration of O–CO bond cleavage in **A3**$^{\bullet+}$ when going to the more polar solvent acetonitrile reflects a slight charge localization in the transition state, presumably in the O–CO bond, similar to the model developed by Kikuchi.[23]

Followup Reactions. The CV investigations also permit a closer analysis of the remaining reaction scheme. While at fast scan rates the reaction system can be described according to a EC_{irr}, at low scan rates the scheme becomes much more complex, which necessitates at least one-electron transfer equilibrium being taken into account as a direct consequence of the concentration dependent crossing effect.[10] In fact, the increasing height of the curve crossing at higher concentrations is consistent with a rate constant on the order of k^f_{DISP} = 10 000 M^{-1} s^{-1} for the forward reaction in the ET equilibrium as written in Figure 10. The corresponding equilibrium constant can be easily determined by the difference of the thermodynamic redox potentials between enol acetate **A3** and benzofuran **B3** as $K_{DISP} = 4 \times 10^{-5}$. Hence, the overall reaction scheme formally can be described as a multiparameter $ECCE_{DISP}$ mechanism.

In order to understand the rate-determining step of this reaction, it is worth looking at the redox behavior of the corresponding radical. The 1,1-dimesityl-3,3-dimethylbuten-2-olate ($E_{1/2}$ = −1.02 V vs Fc) can be oxidized reversibly to the α-carbonyl radical which undergoes further irreversible oxidation at 0.14 V to yield the α-carbonyl cation.[14] According to the irreversibility of this oxidation wave, even at fast scan rates,[14] cyclization is a fast process with respect to the time scale of the experiment and thus cannot be the rate-determining step of the reaction. If the final deprotonation were rate-determining, one would expect effects of acid and base addition onto the benzofuran formation. Since the intensity of curve crossing indicative for benzofuran formed in the CV does not decrease with an increasing acid concentration and does not increase with added base (i.e. collidine), it may be concluded that the [1,2]-methyl shift has to be the rate-determining step with a first-order rate constant of k_{obs} = 0.08 s^{-1}.

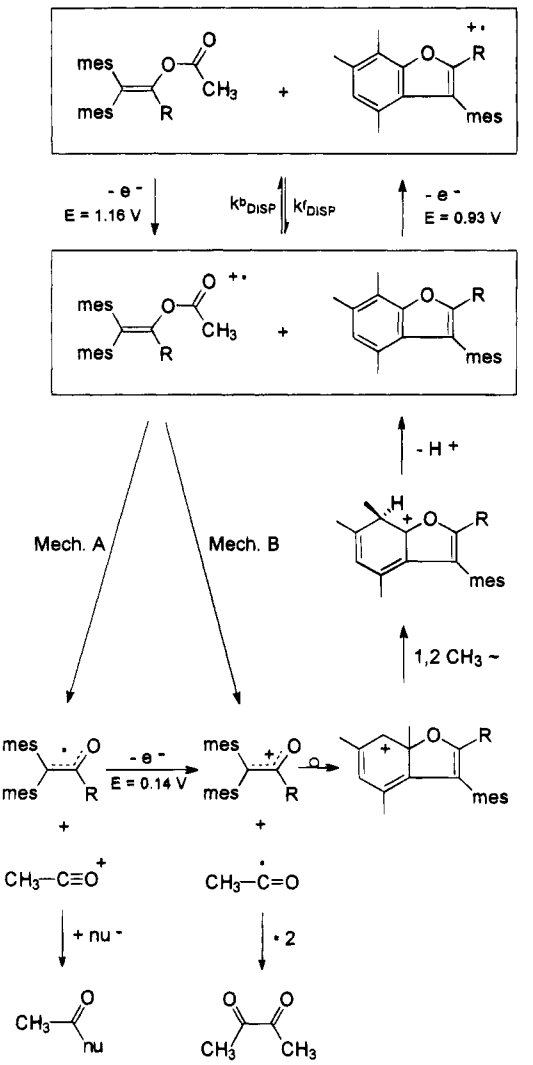

Figure 10. $ECCE_{DISP}$ mechanism of one-electron oxidation of **A3**.

Conclusion. Considering all the information, compelling evidence for the selective cleavage of **A3**$^{\bullet+}$ according to Mech B has been obtained, which should be operative with **A1**, **A2**, and **A4** as well. In terms of using the enol ester functionality as a protecting group, which might be removed through photoinduced one-electron oxidation, bond dissociation according to Mech A would be desirable in order to generate the α-carbonyl radical. Hence, further investigations on this subject, including variations of the ester moiety, are in progress, aiming at speeding up the O–CO bond cleavage with concomitant change in the cleavage selectivity.

Experimental Section

General. Supporting electrolyte Bu_4NPF_6 (Fluka) was electrochemical grade and was recrystallized from ethanol. Acetonitrile and dichloromethane for CV measurements and one-electron oxidation experiments were purified as described

(22) Burghart, A.; Schmittel, M. Unpublished results.
(23) Takahashi, O.; Kikuchi, O. *Tetrahedron Lett.* **1991**, *32*, 4933.

in ref 24. Pyridine was distilled from KOH and ether from sodium. All other materials were of technical quality and were distilled before use. Enols **E1**–**E4** were synthesized as described previously.[24] ^{1}H NMR spectra (250 MHz) were recorded in $CDCl_3$ on a Bruker WM 250 instrument. Chemical shifts are reported in ppm downfield vs internal standard TMS. For quantitative analyses, the internal standard *m*-nitroacetophenone was added. ^{13}C NMR spectra (100 MHz) were recorded on a Bruker AM 400 instrument with internal standard TMS. IR spectra were recorded in KBr using a Perkin-Elmer 421 and 398 spectrometer. Mass spectra were recorded on a Finnigan MAT 44 S mass spectrometer using electron ionization (EI) at 70 eV. Microanalyses were performed on a Perkin-Elmer elemental analyzer 240. Melting points are uncorrected. GC analyses were performed on a Carlo-Erba chromatograph 5300 with an HP 3393 A integrator using a SE30/25 m capillary column. Samples were injected at an injector temperature of 250 °C (split 1:20) and a column temperature of 60 °C. The oven temperature was held for 5 min at 60 °C and then raised to 250 °C at a rate of 10 °C/min. For GC–MS coupling, a Varian 3700 fractometer was used.

General Procedure for the Synthesis of the Enol Acetates A1 and A4 Starting from Enols. Enol **E** (1.3–1.7 mmol) was suspended in acetic anhydride (20 mmol), and pyridine was added dropwise until the enol was completely dissolved. After stirring for 24 h at room temperature, the mixture was poured on ice, 5% HCl (5 mL) was added, and the resulting suspension was extracted three times with ether. The combined organic layers were washed with saturated aqueous $NaHCO_3$ and water and dried over Na_2SO_4. Removal of the solvent and recrystallization from methanol at 8 °C afforded the pure enol esters as white solids.

2,2-Dimesitylethenyl Acetate (A1). Enol **E1** (0.50 g, 1.7 mmol), pyridine (1.0 g, 13 mmol), and acetic anhydride (2.0 g, 20 mmol) yielded 0.49 g (1.5 mmol, 90%) of **A1** as a white solid: mp 130 °C; IR 1750, 1640 cm^{-1}; ^{1}H NMR δ 2.06 (br s, 6 H), 2.10 (s, 3 H), 2.23 (s, 3 H), 2.25 (s, 3 H), 6.82 (s, 4 H), 7.25 (s, 1 H); ^{13}C NMR δ 20.9, 21.0, 121.6, 129.0, 129.7, 132.5, 134.1, 136.5, 137.4, 137.5, 168.1; MS *m/z* 322 (M^+), 281 ($M^+ + 1 - CH_2CO$). Anal. Calcd for $C_{22}H_{26}O_2$ (322.43): C, 81.95; H, 8.13. Found: C, 81.84; H, 7.97.

2,2-Dimesityl-1-phenylethenyl Acetate (A4). Enol **E4** (0.50 g, 1.3 mmol), pyridine (1.0 g, 13 mmol), and acetic anhydride (2.0 g, 20 mmol) afforded 0.40 g (1.0 mmol, 77%) of **A4** as a white solid: mp 185–187 °C; IR 1750, 1600 cm^{-1}; ^{1}H NMR δ 1.72 (s, 3 H), 1.94 (br s, 6 H), 2.13 (s, 3 H), 2.16 (s, 3 H), 6.60 (s, 2 H), 7.06 (m, 5 H); ^{13}C NMR δ 20.7, 20.9, 21.1, 127.9, 128.0, 128.2, 128.6, 129.5, 134.4, 136.0, 136.5, 136.7, 146.2, 169.7; MS *m/z* 398 (M^+), 356 ($M^+ - CH_2CO$). Anal. Calcd for $C_{28}H_{30}O_2$: C, 84.38; H, 7.58. Found: C, 83.88; H, 7.66.

1,1-Dimesitylpropen-2-yl Acetate (A2). Dimesitylketene (5.4 g, 19 mmol) was dissolved in 100 mL of dry ether under a nitrogen atmosphere, and the mixture was cooled to −40 °C. Within 1 h, 14 mL (21 mmol) of a 1.5 M solution of methyllithium in pentane was added under a nitrogen atmosphere, and the mixture was stirred for 3 h. After the mixture was warmed to room temperature, 80 mL of an ethereal solution of acetyl chloride (3.5 g, 56 mmol) was added, and the mixture was stirred for another 2 h. The white solid was filtered off, the filtrate was washed with 5% NaOH, water, saturated $NaHCO_3$, and water and dried, and the solvent was removed. Recrystallization from methanol afforded 4.2 g (13 mmol, 64%) of **A2** as a slightly brown solid: mp 118 °C; IR 1740, 1605 cm^{-1}; ^{1}H NMR δ 1.77 (s, 3 H), 1.82 (s, 3 H), 2.20 (s, 6 H), 2.24 (br s, 6 H), 6.72 (s, 2 H), 6.79 (s, 2 H); ^{13}C NMR δ 18.2, 20.8, 20.9, 126.5, 128.8, 129.1, 133.5, 134.1, 136.0, 136.4, 138.0, 138.5, 145.5, 168.9; MS *m/z* 336 (M^+), 294 ($M^+ - CH_2CO$). Anal. Calcd for $C_{23}H_{28}O_2$: C, 82.10; H, 8.39. Found: C, 81.93; H, 8.39.

2-Acetoxy-1,1-dimesityl-3,3-dimethyl-1-butene (A3). To 100 mL of an ethereal solution of dimesitylketene (4.0 g, 14 mmol) was added 14 mL (21 mmol) of a 1.5 M solution of *t*-BuLi in pentane during 1 h at −40 °C under a nitrogen atomsphere. After the mixture was stirred for 3 h, it was allowed to warm to room temperature, and a solution of acetyl chloride (1.8 g, 22 mmol) in 50 mL of ether was added dropwise. After the mixture was stirred for 1 h, another 1.0 g (13 mmol) of acetyl chloride was added, and the white precipitate was filtered off. The filtrate was washed with 5% NaOH, water, saturated $NaHCO_3$, and water, dried, and concentrated to leave 4.7 g of a red oil which was recrystallized from methanol to yield 2.8 g (51%) of pure **A3** as a slightly brown solid: mp 133 °C; IR 1750, 1605 cm^{-1}; ^{1}H NMR δ 1.03 (s, 9 H), 1.63 (s, 3 H), 1.88 (br s, 6 H), 2.17 (s, 3 H), 2.20 (s, 3 H), 2.42 (br s, 3 H), 2.72 (br s, 3 H), 6.62 (br s, 2 H), 6.81 (br s, 2 H); ^{13}C NMR δ 20.7, 20.8, 20.9, 28.6, 38.8, 124.9, 127.8, 128.2, 130.2, 130.5, 134.8, 135.2, 135.8, 136.3, 138.5, 152.5, 169.5; MS *m/z* 378 (M^+), 336 ($M^+ - CH_2CO$). Anal. Calcd for $C_{26}H_{34}O_2$: C, 82.53; H, 9.05. Found: C, 82.49; H, 9.19.

General Procedure for the One-Electron Oxidations of the Enol Esters. In a glovebox were placed the desired amount of the one-electron oxidant and 50 μmol of the enol acetate into two separate test tubes equipped with stirring rods. At a high-purity argon line, 2 mL of acetonitrile was added in each test tube to dissolve the reactants. The solution of the enol acetate was added dropwise through a syringe to the solution of the one-electron oxidant, and the resulting mixture was stirred overnight. The mixture was quenched with 2 mL of saturated aqueous $NaHCO_3$ and diluted with 10 mL of CH_2Cl_2. The aqueous layer was extracted three times with CH_2Cl_2, and the combined organic layers were washed with saturated aqueous NaCl and water and dried over Na_2SO_4. Removal of the solvent afforded the crude product. In the reactions using $Fe(phen)_3(PF_6)_3$ as oxidant, the residue was extracted with ether and filtered off to separate insoluble iron salts. Product analysis was performed by GC, GC–MS, and ^{1}H NMR. The benzofurans were identified by comparison with data of authentic samples. For the detailed characterization of benzofurans **B1**–**B4**, see ref 24. Brominated benzofurans were identified by GC–MS.

Cyclic Voltammetry. In a glovebox were placed tetra-*n*-butylammonium hexafluorophosphate (232 mg, 600 μmol) and the electroactive species (6 μmol) into a thoroughly dried CV cell. At a high-purity argon line, acetonitrile or dichloromethane (6.0 mL) was added through a gastight syringe, and a 1 mm platinum disk electrode, as the working electrode, and a Pt wire counter electrode as well as a Ag reference electrode were placed into the solution. The cyclic voltammograms were recorded at various scan rates using various starting and reversal potentials. For determination of the oxidation potentials, ferrocene (6 μmol) was added as the internal standard. For fast scan cyclic voltammetry, 385 mg (1.00 mmol) of supporting electrolyte, 50 μmol of substrate, and 5 mL of solvent were employed in the procedure as described before. Fast scan cyclic voltammograms were carried out at 25 μm Au ultramicroelectrodes, a Pt wire serving as the counter electrode and a Ag wire as the reference electrode. CVs were recorded using a Princeton Applied Research model 362 potentiostat with Philips model PM 8271 XYt-recorder for scan rates of <1 V s^{-1}. For fast scan cyclic voltammetry, a Hewlett-Packard model 331A4 function generator was used while connected to a three-electrode potentiostat developed by C. Amatore.[25] Data were recorded by a Hewlett-Packard 54510 A digitizing oscilloscope linked to a 486DX33 computer using the Hewlett-Packard data transfer program Scopelink. The ratios I_{pc}/I_{pa} were determined according to the equation of Nicholson.[26] For fast scan CVs, the graphical method of Bellamy was employed.[27]

Digital Simulations of the Cyclic Voltammograms. The computer simulation of the redox chemistry of the

(24) (a) Röck, M.; Schmittel, M. *J. Prakt. Chem.* **1994**, *336*, 325. (b) Schmittel, M.; Röck, M. *Chem. Ber.* **1992**, *125*, 1611. (c) Schmittel, M.; Baumann, U. *Angew. Chem.* **1990**, *102*, 571; *Angew. Chem., Int. Ed. Engl.* **1990**, *29*, 541.

(25) Amatore, C.; Lefrou, C.; Pflügler, F. *J. Electroanal. Chem. Interfacial Electrochem.* **1989**, *270*, 43.

(26) Nicholson, R. *Anal. Chem.* **1966**, *38*, 1406.

(27) Bellamy, A. J. *J. Electroanal. Chem. Interfacial Electrochem.* **1983**, *151*, 263.

examined compounds was carried out on a 486DX 66 computer using the Crank–Nicholson technique[11] and DigiSim.[28] The simulation of a full-cycle voltammogram consisted of 1000 data points, allowing for acceptable resolution of the experimental cyclic voltammograms. All chemical reactions were assumed to be irreversible first-order processes except the ET equilibrium. With a standard heterogeneous electron transfer rate constant of $k^0_{hetero} = 0.5$ cm s^{-1} and standard diffusion coefficients of $D = 10^{-5}$ cm^2 s^{-1}, the rate constants of the chemical steps were varied to achieve the best possible agreement with the experimental curves.

Electrolysis of A3. In a glovebox were placed Bu_4NPF_6 (1.5 g, 3.9 mmol) and **A3** (0.12 g, 0.32 mmol) in an electrolysis cell, and at a high-purity argon line, 30 mL of CH_2Cl_2 was added. The mixture was electrolyzed at 1.7 V vs Ag at a Pt net at 35 mA. After 20 min, the electrolysis was stopped, and the mixture was hydrolyzed by the addition of 10 mL of saturated $NaHCO_3$ and 5 mL of 2 N NaOH and finally diluted with 50 mL of water. The remaining CH_2Cl_2 was distilled off. After the addition of hydroxylamine hydrochloride and nickel(II) iodide, a red solid consisting of nickel(II) diacetyldioxime precipitated.

(28) (a) Rudolph, M. *J. Electroanal. Chem. Interfacial Electrochem.* **1992**, *338*, 86. (b) Rudolph, M.; Reddy, J. P.; Feldberg, S. W. *Anal. Chem.*, in press, 1994.

Acknowledgment. We gratefully acknowledge the financial support by the Volkswagenstiftung and by the DFG (Graduiertenkolleg). In addition, we are most indebted to the Fonds der Chemischen Industrie for the continuous support of our research.

JO9421844